*Neuroscience* 314 (2016) 160–169

# MICROGLIA AND ASTROCYTE ACTIVATION IN THE FRONTAL CORTEX OF RATS WITH EXPERIMENTAL AUTOIMMUNE ENCEPHALOMYELITIS

**N. L. CHANADAY** [†] **AND G. A. ROTH** [*]

*Centro de Investigaciones en Química Biológica de Córdoba (CIQUIBIC, CONICET-UNC), Departamento de Química Biológica, Facultad de Ciencias Químicas, Universidad Nacional de Córdoba, X5000HUA Córdoba, Argentina*

**Abstract—Experimental autoimmune encephalomyelitis (EAE) is a widely used animal model for the human disease multiple sclerosis (MS), a demyelinating and neurodegenerative pathology of the central nervous system. Both diseases share physiopathological and clinical characteristics, mainly associated with a neuroinflammatory process that leads to a set of motor, sensory, and cognitive symptoms. In MS, gray matter atrophy is related to the emergence of cognitive deficits and contributes to clinical progression. In particular, injury and dysfunction in certain areas of the frontal cortex (FrCx) have been related to the development of cognitive impairments with high incidence, like central fatigue and executive dysfunction. In the present work we show the presence of region-specific microglia and astrocyte activation in the FrCx, during the first hours of acute EAE onset. It is accompanied by the production of the pro-inflammatory cytokines IL-6 and TNF-α, in the absence of detectable leukocyte infiltration. These findings expand previous studies showing presynaptic neural dysfunction occurring at the FrCx and might contribute to the understanding of the mechanisms involved in the genesis and prevalence of common MS symptoms.** 

**Key words: multiple sclerosis, microglia, astrocytes, cytokines, neuroinflammation.**

## INTRODUCTION

Multiple sclerosis (MS) is an autoimmune disease of the central nervous system (CNS) that has unknown etiology and lacks of cure. MS as well as its widely used animal model, experimental autoimmune encephalomyelitis (EAE), are characterized by multifocal inflammation and demyelination, blood–brain barrier disruption, reactive gliosis and degeneration of oligodendrocytes and neurons (Dutta and Trapp, 2011). This leads to a complex and very variable set of motor, sensory and cognitive deficits (Gelfand, 2014). The main determinant of the specific clinical manifestation a patient or animal develops is the localization of the lesion within the CNS (Simmons et al., 2013). Among them, the most common and disabling symptom of MS is cognitive fatigue, affecting around 80% of the patients. It is an overwhelming feeling of mental exhaustion that is related to functional changes in the frontal cortex (FrCx) and/or the basal ganglia, and loss of connectivity between them (Dobryakova et al., 2013). Other common cognitive deficit in MS, present in 50–70% of patients, is executive dysfunction which is also related to alterations in various areas of the FrCx (Cerezo García et al., 2015; Grech et al., 2015).

Classic EAE models can be actively induced in susceptible animals by immunization with whole myelin or specific myelin proteins in an appropriate adjuvant (Degano and Roth, 2000). Although EAE has been widely used to study the molecular and cellular basis of MS, both diseases differ in the pattern of lesion distribution within the CNS (Mix et al., 2008). While most MS patients exhibit lesions primarily in the brain, animals with classic EAE present the majority of inflammatory plaques in spinal cord and optic nerve (Simmons et al., 2013). Nevertheless, given the importance of brain gray matter damage in the genesis and progression of irreversible cognitive impairment in MS, during the last years the occurrence of inflammation and neurodegeneration in different brain areas has been increasingly studied in EAE. Neuroinflammation, demyelination and neurodegeneration in deep brain areas like the striatum and the hippocampus, along with their behavioral correlations, have been profusely examined (Gentile et al., 2015). On the contrary, cortical participation in EAE development has been less investigated, especially the FrCx. Our and other groups have described functional changes in neurons along with glia activation and loss of oligodendrocytes in the brain cortex of animals with EAE (Vilcaes et al., 2009; Girolamo et al.,

[*]Corresponding author. Address: Departamento de Química Biológica-CIQUIBIC, Facultad de Ciencias Químicas, Universidad Nacional de Córdoba, Ciudad Universitaria, Córdoba X5000HUA, Argentina. Tel: +54-351-5353855x3418.
E-mail addresses: nchanaday@gmail.com (N. L. Chanaday), garoth@fcq.unc.edu.ar (G. A. Roth).
[†] Present address: Department of Neuroscience, University of Texas Southwestern Medical Center, Dallas, TX 75390-9111, USA.

*Abbreviations:* ANOVA, analysis of variance; CFA, complete Freund's adjuvant; CNS, central nervous system; DAPI, 4′,6-diamidino-2-pheny lindole; dpi, days post-induction; EAE, experimental autoimmune encephalomyelitis; FrCx, frontal cortex; GFAP, glial fibrillary acidic protein; Iba1, ionized calcium binding adaptor molecule 1; IL, interleukin; mRNA, messenger RNA; MS, multiple sclerosis; PBS, phosphate-buffered saline; PFA, paraformaldehyde; ReCx, remaining portion of the cortex (not frontal); RT-PCR, reverse transcription polymerase chain reaction; TNF, tumor necrosis factor.

http://dx.doi.org/10.1016/j.neuroscience.2015.11.060
0306-4522/

2011; MacKenzie-Graham et al., 2012; Yang et al., 2013). In a previous work using an acute model of EAE, we have demonstrated that presynaptic alterations are concentrated in the frontal region of the cortex (Chanaday et al., 2015). In order to understand the causes of this spatial segregation, and shed light on the origins of highly common MS symptoms like cognitive fatigue and executive dysfunction, herein we continue and deepen that study by analyzing the presence of neuroinflammation in the FrCx.

## EXPERIMENTAL PROCEDURES

### Chemicals

Whole myelin was purified from bovine spinal cords as previously described (Degano and Roth, 2000). Complete Freund's adjuvant (CFA), bovine serum albumin (BSA), paraformaldehyde (PFA), (3-aminopropyl) triethoxysilane, 4′,6-diamidino-2-phenylindole (DAPI) and rabbit polyclonal anti-glial fibrillary acidic protein (GFAP, Cat. No. G9269) were from Sigma–Aldrich Co. (St. Louis, MO, USA). Goat polyclonal anti-ionized calcium binding adaptor molecule 1 (Iba1) antibody (Cat. No. ab107159) was from Abcam (Cambridge, UK). TRIzol® reagent, DNAse I (Cat. No. 18068015) and SYBR Green PCR Master Mix (Cat. No. 4309155) were purchased from Life Technologies (Carlsbad, CA, USA). M-MLV reverse transcriptase (Cat. No. M1705) and recombinant RNasin(R) RNase Inhibitor (Cat. No. N2511) were from Promega Corporation (Madison, WI, USA). Custom PCR primers were ordered from Invitrogen (by Life Technologies, Carlsbad, CA, USA). All other chemicals were analytical grade reagents of the highest purity available.

### Animals and EAE active induction

Albino rats, 40-day-old from a Wistar strain inbred in our laboratory for 40 years were used. All experiments were performed in accordance with the international and institutional guidelines for animal care and the protocol was approved by the local institutional review committee for animal studies (Res. No. 832/2015). Active disease was induced by intradermal injection in both hind feet of 0.5 ml of an emulsion of 0.25-ml phosphate-buffered saline (PBS) and 0.25-ml CFA containing 8-mg bovine myelin (EAE group). Control animals received 0.5 ml of the same emulsion without any antigenic preparation (CFA group). Animals were weighed and examined daily for clinical signs of neurological impairment. Most animals develop only a monophasic course (acute stage, 11–13 days post-induction, dpi) and show spontaneous neurological improvement 2–4 days after the onset of the disease regaining the total ability to walk by 17–18 dpi (Slavin et al., 1996). Clinical severity was scored as follows: 0, no clinical expression of the disease; 0.5, loss of tip tail tonus; 1, flaccid tail; 2, hind limb weakness; 3, complete hind leg paralysis accompanied by urinary incontinence; 4, quadriparesis; 5, moribund state or death.

### Tissue preparation and immunofluorescence

The day of onset of clinical signs, two animals from each experimental group (EAE and CFA) were anesthetized with ketamine:xylazine 3:1 (300 μl/100 g body weight). Two independent experiments were carried out (total $N$ per group = 4). The perfusion was performed with a peristaltic pump P-3 (Pharmacia, Stockholm, Sweden), through the left cardiac ventricle, after occlusion of the descending aorta to only affect the brain. First blood was washed with 0.1 M phosphate buffer at 4 °C and 1000 ml/h for 10 min. Then the tissue was fixed with 4% PFA in phosphate buffer at 4 °C and 600 ml/h for 30 min. Cerebrum, cerebellum and brain stem were extracted from the cranial cavity and post-fixed in 4% PFA in phosphate buffer at 4 °C for 24 h. For cryoprotection, tissues were passed through sucrose solutions of increasing concentrations (15% and 30% in milliQ water) until decantation. Finally, they were embedded in mounting medium Cryoplast® (Biopack, Buenos Aires, Argentina) and stored at −80 °C. Sagittal sections of 20 μm of thickness were cut by cryostat (CM1510 S model, Leica Microsystems, Wetzlar, Germany) and attached to previously silanized glass slides, and stored at −20 °C until use.

For the immunofluorescence assay, cryosections were dried overnight at 37 °C and washed in PBS 3 times for 10 min each. Tissue slices were then permeabilized for 15 min at room temperature with 0.2% Triton X-100 in PBS, and blocked for another 1 h with 4% fetal bovine serum in permeabilization buffer. Then, primary antibodies prepared in blocking buffer (anti-GFAP 1:200, anti-Iba1 1:500) were added and incubated overnight at 4 °C in a humid chamber. Next day the sections were washed with PBS 3 times for 10 min each and labeled for 1 h at room temperature with secondary antibodies (donkey anti-rabbit Alexa Fluor® 488 dil. 1:500, donkey anti-goat Alexa Fluor® 546 dil. 1/500) prepared in PBS. Finally, slices were incubated with DAPI solution for 5 min at room temperature, washed 5 times and mounted using Mowiol mounting medium.

Tissues were viewed and photographed using a FV1000 confocal microscope (Olympus, Tokyo, Japan) equipped with argon/helium/neon lasers and a 60× oil-immersion Zeiss Plan Apochromat objective (NA = 1.42, pixel resolution = 0.20 μm). The $x$–$y$ image size was 1024 × 1024 pixels = 0.02 × 0.02 cm, and 20 × 1 μm thick $z$ stacks were performed (total $z$ distance: 20 μm). Optical sections were projected and the resulting 2D images were analyzed in a blinded fashion employing the ImageJ software (NIH). Sagittal slices at four different laterals were analyzed per animal: 0.5, 1.0, 2.0 and 2.5 mm (according to Paxinos and Watson Atlas, 2007). On each slice, four to five photographs were taken per area. FrCx areas: motor cortex and prefrontal cortex; ReCx areas: parietal, retrosplenial granular, somatosensory and visual cortices. Selection of photographed regions was based on DAPI staining (to avoid subjectivities in the selection of areas based on Iba1 of GFAP fluorescent signals). Number of cells and soma areas were measured by binarizing the images

and counting only somas (particles) that do not intersect the borders (not fragmented).

### RNA purification and cDNA synthesis

Rats from the CFA and EAE groups were euthanized quickly by decapitation and the brains were removed. FrCx (defined as the frontal region of the isocortex from the Bregma 5.5 to 1.0 mm; Paxinos and Watson, 2007) was dissected and snap frozen in liquid nitrogen. The samples were stored at −80 °C until use. Tissues (50–100 mg) were homogenized, resuspended in 1 ml of TRIzol reagent and incubated at room temperature for 5 min. RNA was extracted by adding 0.2 ml of chloroform and centrifugation at 13,800*g* at 4 °C for 15 min. Subsequently, 0.4 ml of the aqueous phase was incubated overnight at −20 °C with 1 ml of isopropanol to allow precipitation of the RNA. The precipitate was washed twice with cold 70% ethanol and resuspended in sterile RNAse-free milliQ water. RNA content and purity were quantified by measuring the absorbance at 260 nm and the ratio of absorbance at 260/280 nm, respectively.

For reverse transcription 1 μg of RNA was incubated at room temperature with DNase I to remove possible contamination with genomic DNA. The product was incubated with random hexamer primers, deoxynucleotides and the reverse transcriptase M-MLV, in the presence of an RNase inhibitor (final volume 25 μl). Reverse transcription was performed following the manufacturer's specifications, employing a thermocycler Mastercycler gradient (Eppendorf, Hamburg, Germany) in one cycle as follows: 6 min at 25 °C, 60 min at 37 °C, 18 min at 70 °C and 10 min at 4 °C. The generated cDNA was diluted to a final volume of 175 μl with sterile milliQ water and stored at −20 °C until use.

### Real-time PCR

In each PCR tube 6 μl of cDNA was mixed with 0.375 μl of a 10 μM solution of each primer (see sequences in Table 1, based in previous works by others, Peinnequin et al., 2004; Bock et al., 2013) and 7.5 μl of 2× SYBR Green PCR Master Mix, to a final volume of 15 μl with sterile milliQ water. Triplicates were prepared for each sample. Real-time PCR was performed on the thermal cycler Rotor-Gene Q (Qiagen, Venlo, Limburg, Netherlands) according to the following protocol: Initial denaturation 10 min at 95 °C, amplification (45 cycles) with denaturation 15 s at 95 °C, annealing 30 s at 60 °C and extension 30 s 70 °C. To confirm the presence of a single product a melting curve of the DNA was always made covering the range of 50–95 °C.

Semi-quantification was performed by the method of ΔΔCt. First, the difference between the Ct value of amplified messenger RNA (mRNA) of interest and Ct value of a constitutive gene expression (GAPDH) was calculated. The difference between the ΔCt obtained for each sample and a reference sample (mean of CFA group) was then calculated (ΔΔCt). Relative gene expression is informed as $2^{-\Delta\Delta Ct}$. The concentration of cDNA and primers, the real-time PCR protocol and the threshold for determining the Ct values were experimentally established using calibration curves (Ct vs log[cDNA concentration]). The selected experimental conditions showed a PCR efficiency of 100 ± 10% for all primers (data not shown).

### Data analysis

Data analysis was performed using Prism (GraphPad Software). Results are expressed as mean ± SEM. For immunofluorescence experiments a two-way analysis of variance (ANOVA) was employed and, if it revealed significant effects ($p \leqslant 0.05$), Bonferroni posttest was used to compare experimental groups for each cortical area. For real-time reverse transcription polymerase chain reaction (RT-PCR) experiments, mRNA levels of a given cortical area from the CFA or EAE group were compared by pairs using Student's *t*-test. In all cases a $p \leqslant 0.05$ was considered to represent a significant difference between groups.

## RESULTS

### Microglia and astrocytes activation at the onset of EAE is concentrated in the frontal region of the cortex

Our group has previously described presynaptic alterations that appear at the onset of acute EAE (first 12–24 h of symptomatic stage) and seemed to be restricted to the frontal region of the cortex (Chanaday et al., 2015). To elucidate the possible causes of these changes, in the present work we examined the activation state of microglia and astrocytes in the cerebral cortex of CFA and EAE animals, with emphasis on the differences, if any, between the frontal region and the rest. A qualitative analysis revealed increased GFAP and Iba1 immunostaining in the FrCx of rats from the EAE group compared to control (Fig. 1). This apparent activation of astrocytes and microglia was more evident in the outer cortical layers (I–III), i.e. closer to the meninges (Fig. 1A, C). In the meninges also, there were Iba1$^+$ rounded cells, most likely meningeal macrophages, present in both CFA and EAE groups (yellow arrow in Fig. 1C) which might result from peripheral inflammation caused by the adjuvant (Schmitt et al., 2012).

On the other hand, in different remaining areas of the cortex (ReCx) there was no or mild activation of the glia in the EAE group, in comparison either to the FrCx or to the CFA group (Fig. 2), implying that at the beginning of the effector phase of acute EAE there might be a regional segregation of changes at the level of the cortex.

To better define and characterize the activation state of microglia and astrocytes, the structure of these cells were studied in detail. One of the most evident markers of microgliosis is the elevation of this cell population, due to both proliferation and blood monocytes recruitment (Wirenfeldt et al., 2007). In the cortex of EAE brains we found increased numbers of Iba1$^+$ cells (about 30%) in both FrCx and ReCx respect to CFA (Fig. 3A). Microglial activation is also tightly related to its morphology. It is now accepted that resting unactivated microglia has a highly dynamic morphology, on average composed by a small cell body or soma and numerous

**Table 1.** Primer sequences, access numbers and amplicon size of the studied mRNAs

| Target | Access number | Primer sequences | | Amplicon size (bp) |
|---|---|---|---|---|
| | | Forward (5′→3′) | Reverse (3′→5′′) | |
| S100B | NM_013191.1 | GGGTCACCTGTAAGAATCAA | GAGGACAAGCAGTTGTAA | 153 |
| GFAP | NM_017009.2 | GACCGCTTTGCTAGCTACATCG | GGTTTCATCTTGGAGCTTCTGC | 246 |
| IL-1β | NW_047658 | CACCTCTCAAGCAGAGCACAG | GGGTTCCATGGTGAAGTCAAC | 79 |
| IL1-R1 | NW_047814.1 | GTTTTTGGAACACCCTTCAGCC | ACGAAGCAGATGAACGGATAGC | 105 |
| IL-6 | M26745 | TCCTACCCCAACTTCCAATGCTC | TTGGATGGTCTTGGTCCTTAGCC | 79 |
| TNF-α | D00475 | AAATGGGCTCCCTCTCATCAGTTC | TCTGCTTGGTGGTTTGCTACGAC | 111 |

narrow, very long and ramified processes (Karperien et al., 2013). Different types and intensities of insults are related to a dramatic remodeling that includes retraction and thickening of the processes, and size increase and deformation of the cell soma, leading to an ameboid and/or rounded appearance at extreme activation cases (i.e. reactive microglia). The morphometric assessment of microglia was performed based on previous descriptions by others (Jonas et al., 2012; Torres-Platas et al., 2014). In the whole cortex (FrCx and ReCx) of animals from the CFA group we found microglia with the resting phenotype, classified as stage 1 (based on Jonas et al., 2012) as well as some intermediate, slightly activated microglia (mostly in stage 2 and rarely in stage 3, Fig. 3F). As mentioned before, this could be caused by the sustained peripheral inflammation triggered by the complete adjuvant. Besides these two phenotypes, in the cortex of the EAE group we found microglia in stages 3 and 4, and a few in stage 5, mainly perivascular or perimeningeal. The relative amount of the activated subpopulation was higher in the FrCx than in the ReCx (data not shown). To quantify this qualitative observation, we measure classic morphometric parameters (Torres-Platas et al., 2014). In the cortex of EAE animals the soma size (area) of Iba1$^+$ cells was bigger than in the CFA group, being this change more obvious in the FrCx (Fig. 3B). Furthermore, microglia in the FrCx of the EAE group, but not in the ReCx or in the control group, presented fewer number of processes, which were significantly shorter and thicker (Fig. 3C–E). These results suggest the occurrence of more intense microglial activation in the FrCx, compared to the ReCx, during the first hours of the symptomatic stage of acute EAE.

On the other hand, astrocyte hypertrophy and glial scar formation was one of the first discovered features of MS lesions (Brosnan and Raine, 2013). As for microglia, the extent and type of structural and functional alterations that astrocytes undergo depend on the nature and intensity of the insult. Activation of astrocytes leads to disruption of their essential CNS functions, like blood–brain barrier formation, synaptic transmission strengthening and neuron nurture, as well as secretion of inflammatory cytokines and chemokines that are vital for the recruitment of blood leukocytes and the expansion and worsening of lesions (Brosnan and Raine, 2013; Brambilla et al., 2014). The day of acute EAE onset, the number of GFAP$^+$ cells in the cortex was considerably increased, compared to the CFA group (Fig. 4A). This increment was larger in the FrCx, about at 100% compared to a 50% rise in the ReCx. Moreover, only in the FrCx we found a significant thickening of astrocytic main processes, (about 30%; Fig. 4B). Similar to that observed for microglia, activation of astrocytes seems to be concentrated in the frontal region of the cortex, at least at this early stage of the symptomatic phase of acute EAE.

### Expression of neuroinflammatory molecules is elevated specifically in the frontal region of the cortex

As cited previously, cytokine secretion by activated glial cells is crucial for the process of infiltration (Rodgers and Miller, 2012). With the aim of confirming our immunofluorescence findings, mRNA levels of key cytokines were measured by real-time RT-PCR. While in the ReCx mRNA levels of all tested messengers were similar between CFA and EAE groups (Fig. 5B), expression of the pro-inflammatory cytokines tumor necrosis factor α (TNF-α) and interleukin 6 (IL-6) were increased in the FrCx about five- and twofold, respectively (Fig. 5A). Another pro-inflammatory cytokine relevant in this model, IL-1β (Matsuki et al., 2006), and its receptor were not affected at this stage of acute EAE. Neither was S100B, a neurotrophic protein reported to be augmented during classic astrocyte activation (Liao et al., 2008).

Reinforcing the morphometric analysis that revealed astrocyte activation, GFAP mRNA showed a threefold increase in the FrCx of rats with EAE, compared to control (Fig. 5A). Therefore, these results indicate that presynaptic alterations described previously by our group could be caused, at least in part, by activation of microglia and astrocytes in the FrCx. However, with these studies we cannot elucidate the foundations of this regional segregation during the first hours of the effector stage of acute EAE. In this regard, we would like to mention that at the same time-point, we did not find leukocyte infiltration into the brain cortex either by classic histopathological studies (Hematoxylin–Eosin and Toluidine Blue stains) or by isolation of CNS-infiltrating mononuclear cells followed by flow cytometry characterization, while these assays are positive for infiltration in the spinal cord of EAE rats (Bibolini et al., 2014). Also, we did not detect the presence of neuron degeneration by Fluoro-Jade® B stain in the FrCx or the ReCx (data not shown).

## DISCUSSION

In the present work we describe the presence of region-specific neuroinflammation in the frontal portion of the cortex, during the first hours of acute EAE onset.

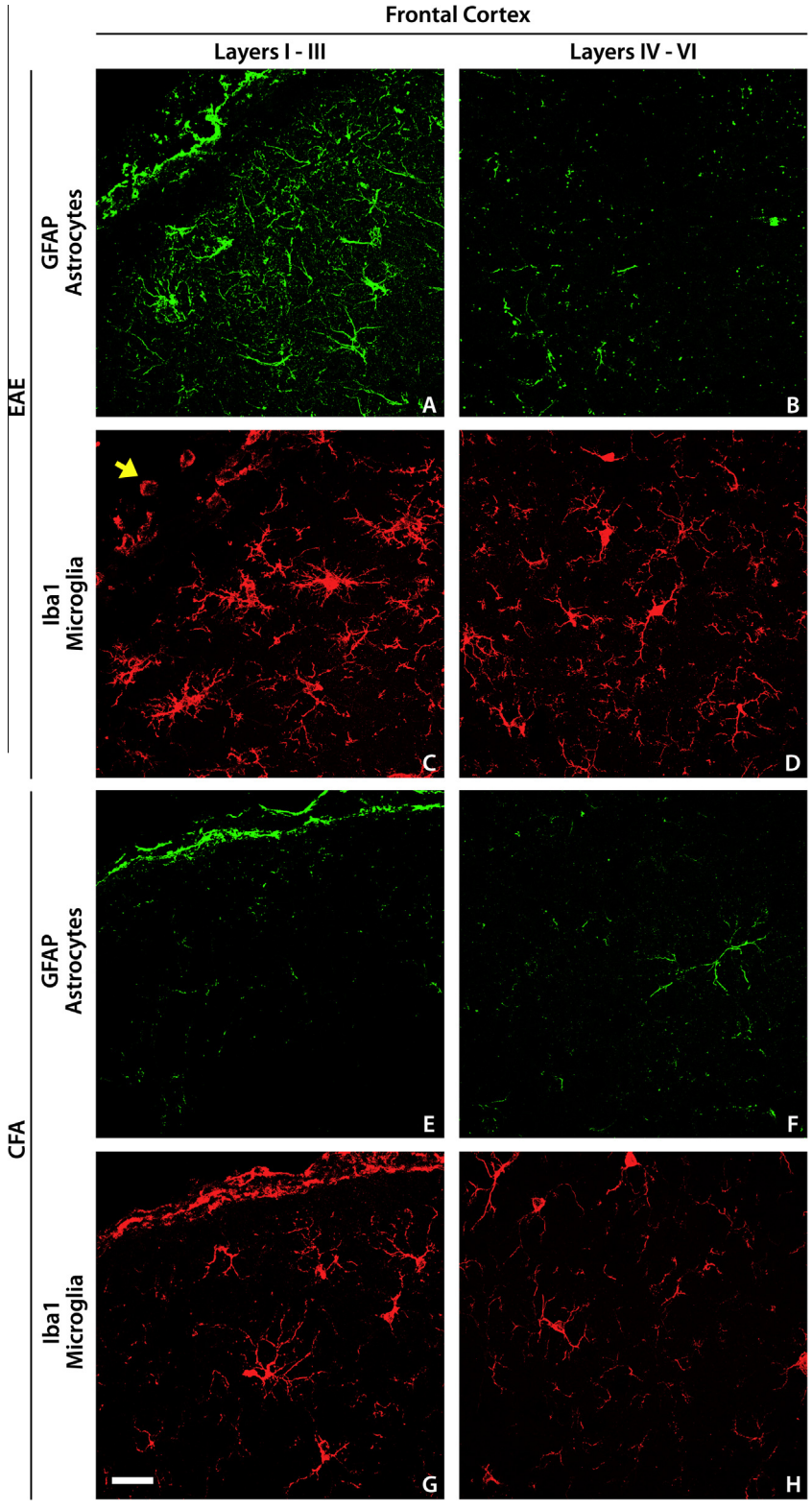


**Fig. 1.** Representative immunofluorescence images from FrCx of Iba1+ (red) and GFAP+ (green) cells, i.e. microglia and astrocytes, respectively. The frontal cortex was defined as the frontal region of the isocortex from the Bregma 5.5 to 1.0 mm, and it contained: the primary and secondary motor cortices (analyzed at laterals 2.0 and 2.5), and the prefrontal cortex (analyzed at laterals 0.5 and 1.0; including orbitofrontal, cingulate, prelimbic and infralimbic cortices). All sub-areas were pooled into one group: FrCx. Yellow arrow: Iba1+ rounded cells in the meninges. White bar = 25 μm.

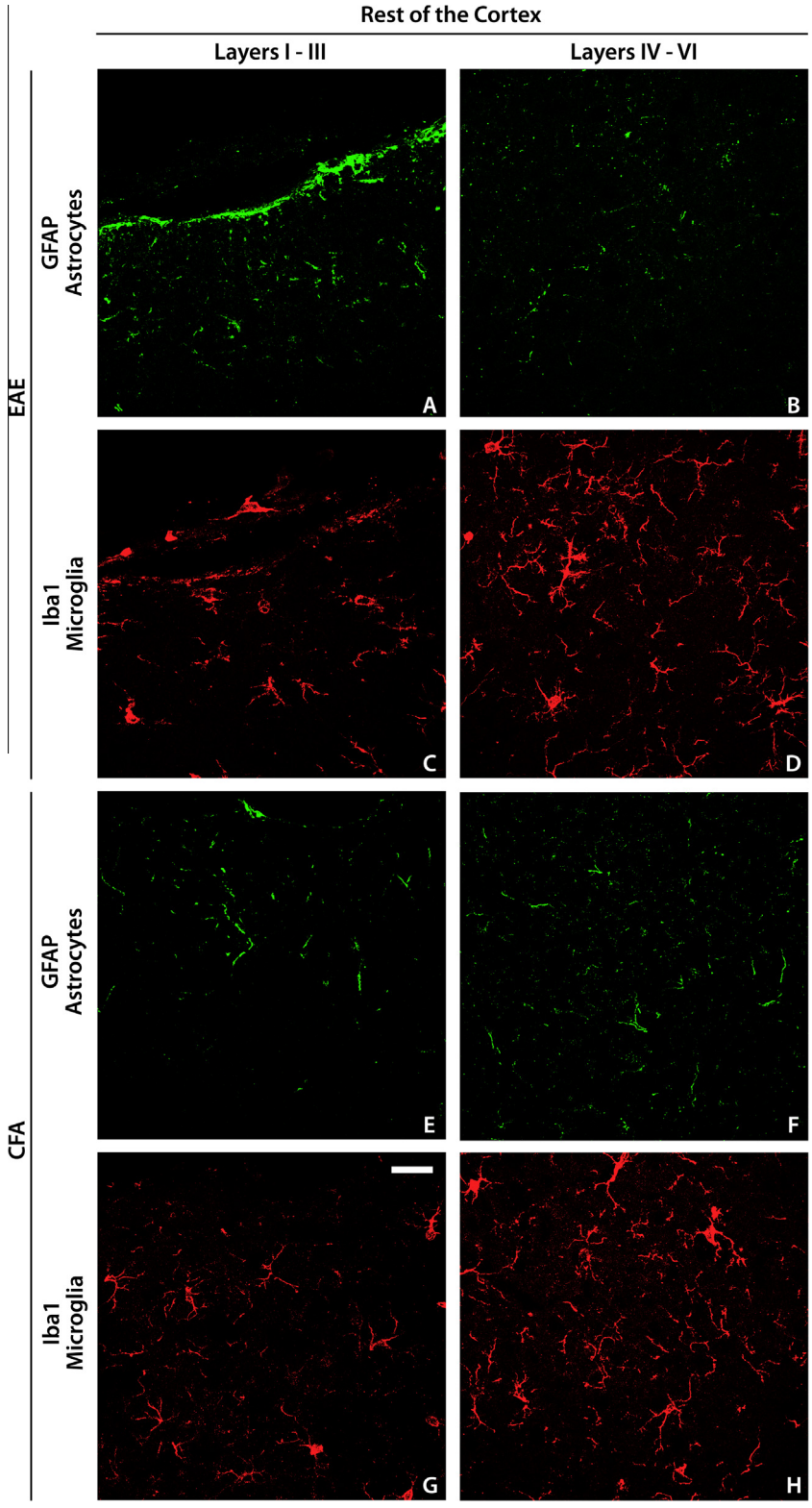


**Fig. 2.** Representative immunofluorescence images from ReCx of Iba1+ (red) and GFAP+ (green) cells, i.e. microglia and astrocytes, respectively (representative images from the primary sensory cortex). The following areas were analyzed: parietal cortex, retrosplenial granular cortex, primary somatosensory cortex and primary and secondary visual cortices (all areas showed similar immunofluorescence signals, they were pooled together as ReCx for statistical analysis). White bar = 25 μm.

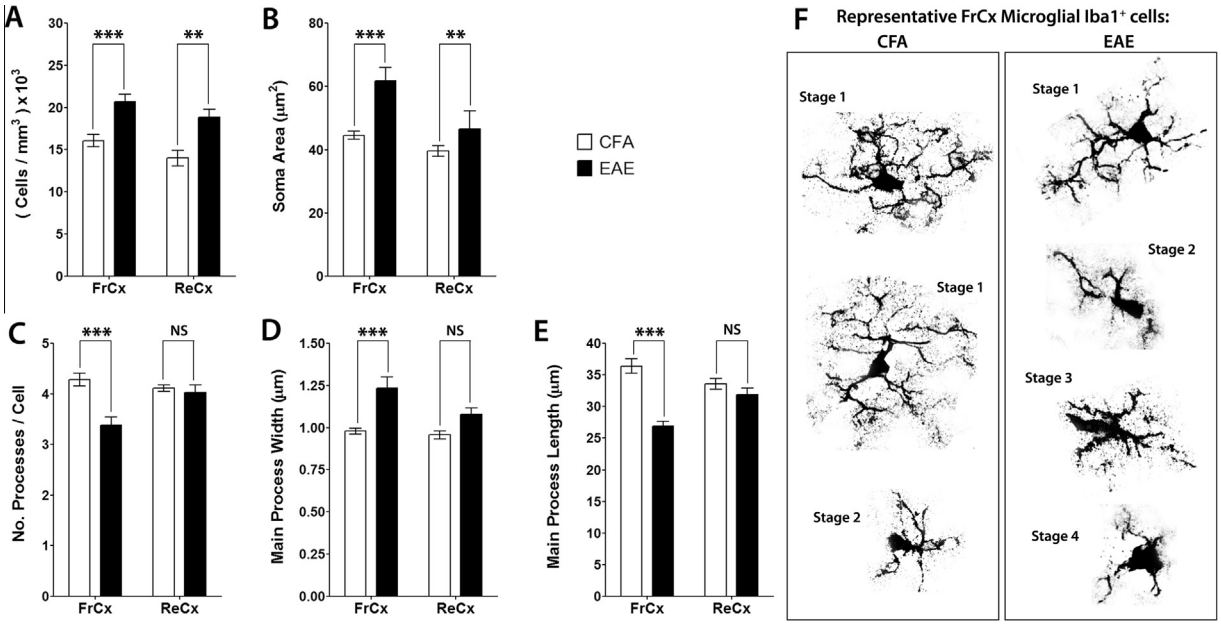


**Fig. 3.** Morphometric analysis of cortical (FrCx and ReCx) Iba1$^+$ microglial cells, in control (CFA) and EAE groups. (A) Total amount (number) of cells per area. 16.1 ± 0.7 and 14.9 ± 0.9 cells × $10^3$/mm$^3$ in FrCx and ReCx of CFA group, respectively; 20.7 ± 0.9 and 18.8 ± 0.9 cells × $10^3$/mm$^3$ in FrCx and ReCx of EAE group, respectively. (B) 2D cell body size (soma area). 44.5 ± 1.2 and 39.6 ± 1.5 μm$^2$ in FrCx and ReCx of CFA group, respectively; 61.8 ± 4.2 and 46.5 ± 5.5 μm$^2$ in FrCx and ReCx of EAE group, respectively. (C) Quantity (number) of processes emanating from the soma per cell. 4.3 ± 0.1 and 4.1 ± 0.1 processes/cell in FrCx and ReCx of CFA group, respectively; 3.4 ± 0.2 and 4.0 ± 0.2 processes/cell in FrCx and ReCx of EAE group, respectively. (D) Width of the main processes in the proximity of the soma. 0.98 ± 0.02 and 0.96 ± 0.02 μm in FrCx and ReCx of CFA group, respectively; 1.23 ± 0.05 and 1.08 ± 0.04 μm in FrCx and ReCx of EAE group, respectively. (E) Total length of the longest main process of each cell. 36.4 ± 1.2 and 33.6 ± 0.8 μm in FrCx and ReCx of CFA group, respectively; 26.8 ± 0.8 and 31.9 ± 1.0 μm in FrCx and ReCx of EAE group, respectively. (F) Representative Iba1$^+$ cells most frequently found in the FrCx of each experimental group. Data from two independent experiments ($N$ = 4 rats per group, 45–55 cells per animal were analyzed) and expressed as mean ± SEM (NS = not significant; $^*p \leqslant 0.05$; $^{**}p \leqslant 0.01$; $^{***}p \leqslant 0.001$; two-way ANOVA with Bonferroni posttest).

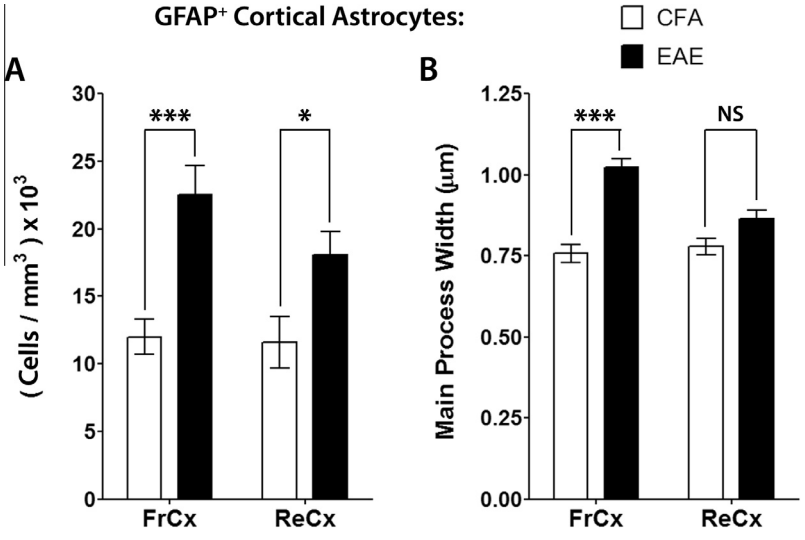


**Fig. 4.** Morphometric analysis of cortical (FrCx and ReCx) GFAP$^+$ astrocytes, in control (CFA) and EAE groups. (A) Total amount (number) of cells per area. 12.0 ± 1.3 and 11.6 ± 1.8 cells × $10^3$/mm$^3$ in FrCx and ReCx of CFA group, respectively; 22.5 ± 2.2 and 18.1 ± 1.6 cells × $10^3$/mm$^3$ in FrCx and ReCx of EAE group, respectively. (B) Width of the main processes in the proximity of the soma. 0.76 ± 0.03 and 0.78 ± 0.03 μm in FrCx and ReCx of CFA group, respectively; 1.02 ± 0.03 and 0.86 ± 0.03 μm in FrCx and ReCx of EAE group, respectively. Data from two independent experiments ($N$ = 4 rats per group, 25–35 cells per animal were analyzed) and expressed as mean ± SEM (NS = not significant; $^*p \leqslant 0.05$; $^{**}p \leqslant 0.01$; $^{***}p \leqslant 0.001$; two-way ANOVA with Bonferroni posttest).

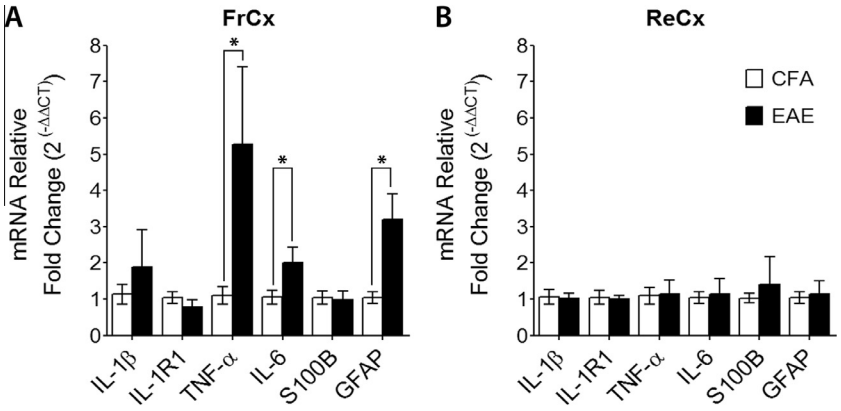


**Fig. 5.** mRNA relative levels of relevant pro-inflammatory cytokines and markers. (A) mRNA levels in the FrCx of CFA and EAE groups. TNF-α: 1.1 ± 0.2 and 5.3 ± 2.1; IL-6: 1.1 ± 0.2 and 2.0 ± 0.4, GFAP: 1.0 ± 0.2 and 3.2 ± 0.7; for CFA and EAE groups, respectively. (B) mRNA levels in the ReCx of CFA and EAE groups. Data from two independent experiments ($N = 4$ rats per group) and expressed as mean ± SEM ($^{*}p \leqslant 0.05$, paired groups were compared using *t*-test).

It comprises activation of microglia and astrocytes, in the absence of detectable leukocyte infiltration. These findings support previous studies form our laboratory showing presynaptic neural dysfunction at the beginning of the effector phase of EAE, also concentrated at the FrCx (Cid et al., 2011; Chanaday et al., 2015).

MS physiopathology and treatment response is highly heterogeneous among patients, and depends on the localization and severity of the lesions within the CNS (Simmons et al., 2013). Cognitive decline occurs in more than half of patients and is thought to be the consequence of neuron and oligodendrocyte degeneration cause by neuroinflammation (Jonas et al., 2014). Particularly, alterations in the functionality and/or connectivity of the FrCx are related to the development of the most common and disabling cognitive symptom of MS, central fatigue, which affects around 80% of patients (Dobryakova et al., 2013). Executive dysfunction also has a high incidence in MS, and is related to changes in the activation and the presence of lesions in the prefrontal region of the FrCx (Cerezo García et al., 2015; Grech et al., 2015). Beyond some anatomical differences, human, macaque and rat frontal lobes share functional properties and network connectivity (Seamans et al., 2008; Wallis, 2012). In rodent models of EAE the brain cortex has not been as extensively studied as in MS. There are reports of progressive synaptic, dendritic and neuronal loss in the cortex of mice with chronic EAE, accompanied by reduction of whole cortical volume (MacKenzie-Graham et al., 2012; Spence et al., 2014). Using the same chronic model other authors found activated microglia and infiltrating macrophages, along with demyelination, oligodendrocyte loss and failure in oligodendroglial precursor maturation in several cortical areas, including the FrCx (Girolamo et al., 2011). All the alterations mentioned were analyzed in the chronic phase of EAE, between 5 and 70 days after onset, when clinical signs are clearly established. On the other hand, during the pre-symptomatic stage of EAE (around 2 days before the onset) behavioral alterations and instability of synaptic contacts in the somatosensory cortex has been informed to occur in the absence of demyelination, glia activation or leukocyte infiltration, being these changes dependent on the presence of circulating TNF-α due to the peripheral inflammation (Acharjee et al., 2013; Yang et al., 2013). The present work was performed within the first hours of appearance of clinical signs, around the first 12 h of EAE onset. In accordance with the mentioned antecedents, we found an in-between scene, where there was not leukocyte infiltration yet but microglia and astrocyte activation was beginning since we observed an intermediate activation state. As we have previously reported for presynaptic functional and morphological alterations (Chanaday et al., 2015), this glial activation is concentrated in the FrCx, leading us to think that neuroinflammation could be responsible for the impairments in neurotransmission.

Besides the increase in GFAP mRNA expression, which reinforces the histologically defined astrocytic activation, we detected elevations in the levels of the pro-inflammatory cytokines TNF-α and IL-6 mRNAs. TNF-α, and other inflammatory molecules and cells have been found increased in blood and cerebrospinal fluid by other authors, as a result of the sustained peripheral inflammatory stimulus given by the adjuvant (Schmitt et al., 2012). TNF-α can cross the blood–brain barrier and, once in the brain, it acts upon neurons affecting the neurotransmission and upon microglia inducing its activation, exacerbating the processes of neuroinflammation and excitotoxicity (Montgomery and Bowers, 2012). On the other hand, IL-6 secreted by activated astrocytes, but not by peripheral leukocytes, is essential for leukocyte recruitment and infiltration. It also mediates microglia activation and blood–brain barrier disruption (Linker et al., 2008). IL-6 knock-out animals are resistant to EAE, either if the silencing occurs in the whole organism or if it is restricted to astrocytes (Giralt et al., 2013). These antecedents along with our results indicate that inflammatory mediators reach the FrCx and activate microglial and astroglial cells triggering their morphological remodeling and the local production of TNF-α and IL-6, probably accompanied by chemokines, glutamate and other toxic components. The mentioned inflammatory mediators possibly arrive through the cerebrospinal fluid, given that the activation was more intense in the vicinity of the

meninges, although we cannot discern the reason for this spatial segregation.

In previous reports we showed alterations in the presynaptic release machinery and reduced release of the excitatory neurotransmitter glutamate, along with changes in the GABAergic regulation of this process (Vilcaes et al., 2009; Cid et al., 2011; Chanaday et al., 2015). These changes also appeared in the first hours of EAE onset and were concentrated in the FrCx. In those experiments, neuronal levels of the kinase Erk1/2 and the $Ca^{+}$-dependent phosphatase calcineurin were significantly increased. Interestingly, the expression and activity of these enzymes is highly modulated by IL-6 and TNF-α, respectively (Álvarez et al., 2011; Fang et al., 2013). The activation of microglia and astrocytes herein described might be triggering Erk1/2 and calcineurin pathways in neurons leading to synaptic dysfunction.

## CONCLUSIONS

The present work documented the presence of region-specific activation of microglia and astrocytes in the FrCx of animals at onset of acute EAE. This was accompanied by secretion of pro-inflammatory cytokines, in the absence of leukocyte infiltration. We cannot rule out if oligodendrocytes and myelin are affected at this early stage. Taking into account the high incidence of FrCx lesions in patients with MS and its close relationship to the establishment of irreversible cognitive impairment and the decrease in the quality of life, our studies could contribute to the understanding of the mechanisms involved in the genesis and prevalence of these symptoms. Future efforts are directed to find the clinical correlates of FrCx alterations in different EAE models and the developing of related therapeutic approaches.

## CONFLICT OF INTEREST

The authors declare that they have no conflict of interest.

*Acknowledgments—We thank Dr. Soledad de Olmos for the Fluoro-Jade® B stain and Drs. Cecilia Sampedro and Carlos Mas for guiding us with microscope handling and image analysis. This work was supported by Consejo de Investigaciones Científicas y Técnicas (CONICET), Agencia Nacional de Promoción Científica y Tecnológica (Préstamo BID, PICT 2011-0799), and Secretaría de Ciencia y Tecnología de la Universidad Nacional de Córdoba (SeCyT-UNC), Argentina. N.L.C. is a fellow and G.A.R. is a senior career investigator, all from CONICET.*

## REFERENCES

Acharjee S, Nayani N, Tsutsui M, Hill MN, Ousman SS, Pittman QJ (2013) Altered cognitive-emotional behavior in early experimental autoimmune encephalitis-cytokine and hormonal correlates. Brain Behav Immun 33:164–172.

Álvarez S, Blanco A, Fresno M, Muñoz-Fernández MÁ (2011) TNF-α contributes to caspase-3 independent apoptosis in neuroblastoma cells: role of NFAT. PLoS One 6:e16100.

Bibolini MJ, Scerbo MJ, Roth GA, Monferran CG (2014) Treatment with a hybrid between the synapsin ABC domains and the B subunit of *E. coli* heat-labile toxin reduces frequency of proinflammatory cells and cytokines in the central nervous system of rats with EAE. Neuroscience 277:217–228.

Bock N, Koc E, Alter H, Roessner V, Becker A, Rothenberger A, Manzke T (2013) Chronic fluoxetine treatment changes S100B expression during postnatal rat brain development. J Child Adolesc Psychopharmacol 23:481–489.

Brambilla R, Morton PD, Ashbaugh JJ, Karmally S, Lambertsen KL, Bethea JR (2014) Astrocytes play a key role in EAE pathophysiology by orchestrating in the CNS the inflammatory response of resident and peripheral immune cells and by suppressing remyelination: astrocytes play a key role in EAE pathology. Glia 62:452–467.

Brosnan CF, Raine CS (2013) The astrocyte in multiple sclerosis revisited. Glia 61:453–465.

Cerezo García M, Martín Plasencia P, Aladro Benito Y (2015) Alteration profile of executive functions in multiple sclerosis. Acta Neurol Scand 131:313–320.

Chanaday NL, Vilcaes AA, de Paul AL, Torres AI, Degano AL, Roth GA (2015) Glutamate release machinery is altered in the frontal cortex of rats with experimental autoimmune encephalomyelitis. Mol Neurobiol 51:1353–1367.

Cid MP, Vilcaes AA, Rupil LL, Salvatierra NA, Roth GA (2011) Participation of the GABAergic system on the glutamate release of frontal cortex synaptosomes from Wistar rats with experimental autoimmune encephalomyelitis. Neuroscience 189:337–344.

Degano AL, Roth GA (2000) Passive transfer of experimental autoimmune encephalomyelitis in Wistar rats: dissociation of clinical symptoms and biochemical alterations. J Neurosci Res 59:283–290.

Dobryakova E, DeLuca J, Genova HM, Wylie GR (2013) Neural correlates of cognitive fatigue: cortico-striatal circuitry and effort-reward imbalance. J Int Neuropsychol Soc 19:849–853.

Dutta R, Trapp BD (2011) Mechanisms of neuronal dysfunction and degeneration in multiple sclerosis. Prog Neurobiol 93:1–12.

Fang X-X, Jiang X-L, Han X-H, Peng Y-P, Qiu Y-H (2013) Neuroprotection of interleukin-6 against NMDA-induced neurotoxicity is mediated by JAK/STAT3, MAPK/ERK, and PI3K/AKT signaling pathways. Cell Mol Neurobiol 33:241–251.

Gelfand JM (2014) Multiple sclerosis: diagnosis, differential diagnosis, and clinical presentation. Handb Clin Neurol 122:269–290.

Gentile A, Fresegna D, Federici M, Musella A, Rizzo FR, Sepman H, Bullitta S, De Vito F, Haji N, Rossi S, Mercuri NB, Usiello A, Mandolesi G, Centonze D (2015) Dopaminergic dysfunction is associated with IL-1β-dependent mood alterations in experimental autoimmune encephalomyelitis. Neurobiol Dis 74:347–358.

Giralt M, Ramos R, Quintana A, Ferrer B, Erta M, Castro-Freire M, Comes G, Sanz E, Unzeta M, Pifarré P, García A, Campbell IL, Hidalgo J (2013) Induction of atypical EAE mediated by transgenic production of IL-6 in astrocytes in the absence of systemic IL-6. Glia 61:587–600.

Girolamo F, Ferrara G, Strippoli M, Rizzi M, Errede M, Trojano M, Perris R, Roncali L, Svelto M, Mennini T, Virgintino D (2011) Cerebral cortex demyelination and oligodendrocyte precursor response to experimental autoimmune encephalomyelitis. Neurobiol Dis 43:678–689.

Grech LB, Kiropoulos LA, Kirby KM, Butler E, Paine M, Hester R (2015) The effect of executive function on stress, depression, anxiety, and quality of life in multiple sclerosis. J Clin Exp Neuropsychol 37:549–562.

Jonas RA, Yuan T-F, Liang Y-X, Jonas JB, Tay DKC, Ellis-Behnke RG (2012) The spider effect: morphological and orienting classification of microglia in response to stimuli in vivo. PLoS One 7:e30763.

Jonas A, Thiem S, Kuhlmann T, Wagener R, Aszodi A, Nowell C, Hagemeier K, Laverick L, Perreau V, Jokubaitis V, Emery B, Kilpatrick T, Butzkueven H, Gresle M (2014) Axonally derived matrilin-2 induces proinflammatory responses that exacerbate autoimmune neuroinflammation. J Clin Invest 124:5042–5056.

Karperien A, Ahammer H, Jelinek HF (2013) Quantitating the subtleties of microglial morphology with fractal analysis. Front Cell Neurosci 7:3.

Liao C-W, Fan C-K, Kao T-C, Ji D-D, Su K-E, Lin Y-H, Cho W-L (2008) Brain injury-associated biomarkers of TGF-beta1, S100B, GFAP, NF-L, tTG, AbetaPP, and tau were concomitantly enhanced and the UPS was impaired during acute brain injury caused by *Toxocara canis* in mice. BMC Infect Dis 8:84.

Linker RA, Lühder F, Kallen K-J, Lee D-H, Engelhardt B, Rose-John S, Gold R (2008) IL-6 transsignalling modulates the early effector phase of EAE and targets the blood–brain barrier. J Neuroimmunol 205:64–72.

MacKenzie-Graham A, Rinek GA, Avedisian A, Gold SM, Frew AJ, Aguilar C, Lin DR, Umeda E, Voskuhl RR, Alger JR (2012) Cortical atrophy in experimental autoimmune encephalomyelitis: in vivo imaging. Neuroimage 60:95–104.

Matsuki T, Nakae S, Sudo K, Horai R, Iwakura Y (2006) Abnormal T cell activation caused by the imbalance of the IL-1/IL-1R antagonist system is responsible for the development of experimental autoimmune encephalomyelitis. Int Immunol 18:399–407.

Mix E, Meyer-Rienecker H, Zettl UK (2008) Animal models of multiple sclerosis for the development and validation of novel therapies – potential and limitations. J Neurol 255:7–14.

Montgomery SL, Bowers WJ (2012) Tumor necrosis factor-alpha and the roles it plays in homeostatic and degenerative processes within the central nervous system. J Neuroimmune Pharmacol 7:42–59.

Paxinos G, Watson C (2007) The rat brain in stereotaxic coordinates. Elsevier Inc.

Peinnequin A, Mouret C, Birot O, Alonso A, Mathieu J, Clarençon D, Agay D, Chancerelle Y, Multon E (2004) Rat pro-inflammatory cytokine and cytokine related mRNA quantification by real-time polymerase chain reaction using SYBR green. BMC Immunol 5:3.

Rodgers JM, Miller SD (2012) Cytokine control of inflammation and repair in the pathology of multiple sclerosis. Yale J Biol Med 85:447–468.

Schmitt C, Strazielle N, Ghersi-Egea J-F (2012) Brain leukocyte infiltration initiated by peripheral inflammation or experimental autoimmune encephalomyelitis occurs through pathways connected to the CSF-filled compartments of the forebrain and midbrain. J Neuroinflammation 9:187.

Seamans JK, Lapish CC, Durstewitz D (2008) Comparing the prefrontal cortex of rats and primates: insights from electrophysiology. Neurotox Res 14:249–262.

Simmons SB, Pierson ER, Lee SY, Goverman JM (2013) Modeling the heterogeneity of multiple sclerosis in animals. Trends Immunol 34:410–422.

Slavin DA, Bucher AE, Degano AL, Soria NW, Roth GA (1996) Time course of biochemical and immunohistological alterations during experimental allergic encephalomyelitis. Neurochem Int 29:597–605.

Spence RD, Kurth F, Itoh N, Mongerson CRL, Wailes SH, Peng MS, MacKenzie-Graham AJ (2014) Bringing CLARITY to gray matter atrophy. Neuroimage 101:625–632.

Torres-Platas SG, Comeau S, Rachalski A, Bo GD, Cruceanu C, Turecki G, Giros B, Mechawar N (2014) Morphometric characterization of microglial phenotypes in human cerebral cortex. J Neuroinflammation 11:12.

Vilcaes AA, Furlan G, Roth GA (2009) Inhibition of Ca(2+)-dependent glutamate release from cerebral cortex synaptosomes of rats with experimental autoimmune encephalomyelitis. J Neurochem 108:881–890.

Wallis JD (2012) Cross-species studies of orbitofrontal cortex and value-based decision-making. Nat Neurosci 15:13–19.

Wirenfeldt M, Dissing-Olesen L, Babcock AA, Nielsen M, Meldgaard M, Zimmer J, Azcoitia I, Leslie RGQ, Dagnaes-Hansen F, Finsen B (2007) Population control of resident and immigrant microglia by mitosis and apoptosis. Am J Pathol 171:617–631.

Yang G, Parkhurst CN, Hayes S, Gan W-B (2013) Peripheral elevation of TNF-α leads to early synaptic abnormalities in the mouse somatosensory cortex in experimental autoimmune encephalomyelitis. Proc Natl Acad Sci U S A 110:10306–10311.

*(Accepted 25 November 2015)*
*(Available online 8 December 2015)*